

PFC/JA-85-12

ANALYTIC MIRROR EQUILIBRIA

WITH NEW LONG-THIN TERMS

Daniel L. Goodman  
Jeffrey P. Freidberg  
Barton Lane

Plasma Fusion Center  
Massachusetts Institute of Technology  
Cambridge, Massachusetts 02139 USA

April 1985

## I. Abstract

An analytic equilibrium for a tandem mirror with quadrupole symmetry is derived. We simultaneously expand in  $\beta$  (plasma pressure / magnetic pressure) and  $\lambda$  (long-thin parameter) using a maximal ordering so that both effects enter competitively. These new long-thin corrections extend the results of Pearlstein, et al<sup>1,2</sup>, and can be shown in some cases to be the dominant terms. The new terms make the flux surfaces more diamond shaped than previously thought, and change the scaling of the flux surface distortions with  $\beta$ . Using model pressure and field profiles, simple analytic expressions for the new corrections and flux surface are found and compared with the results of the VEPEC 3D equilibrium code.<sup>3</sup> For the Constance mirror we find good agreement with the code for flux surface shapes and  $\beta$  scaling.

## II. Equilibria Equations

We consider the equilibrium of a non-axisymmetric tandem mirror described by the tensor magnetostatic equations given by

$$\begin{aligned}\nabla_{\perp}(p_{\perp} + B^2/2) - Q \kappa &= 0 \\ \partial p_{\parallel} / \partial B &= p_{\parallel} - p_{\perp} / B \\ \mathbf{J} &= \nabla \times \mathbf{B} \\ \nabla \cdot \mathbf{B} &= 0\end{aligned}\tag{1}$$

where  $Q = B^2 + p_{\perp} - p_{\parallel}$ ,  $\kappa = \mathbf{b} \cdot \nabla \mathbf{b}$ ,  $\mathbf{b} = \mathbf{B}/B$ . The pressures  $p_{\perp}$  and  $p_{\parallel}$  are assumed to satisfy the isorropic conditions:  $p_{\perp}(\psi, B)$ ,  $p_{\parallel}(\psi, B)$  with  $\psi$  the total magnetic flux.

This is a specialization of the general situation in which  $p_{\perp} = p_{\perp}(\psi, \theta, B)$ ,  $p_{\parallel} = p_{\parallel}(\psi, \theta, B)$  where  $\psi$  and  $\theta$  are flux coordinates related to the magnetic field by

$$\mathbf{B} = \nabla \psi \times \nabla \theta\tag{2}$$

The analysis also requires an explicit expression for  $J_{\parallel}$ . This expression, known as the parallel current relationship (obtained by setting  $\nabla \cdot \mathbf{J} = 0$  and solving for  $J_{\parallel}$ ) is given by

$$\mathbf{b} \cdot \nabla (Q J_{\parallel} / B^3) = 1/B^2 \mathbf{b} \cdot (\nabla (p_{\perp} + p_{\parallel}) \times \kappa)\tag{3}$$

In order to obtain non-axisymmetric equilibria, we simultaneously expand in  $\beta$  (plasma pressure / magnetic pressure) and  $\lambda$  (long thin

parameter) using a maximal ordering so that both effects enter competitively. If  $\lambda$  is treated as the basic ordering parameter, then the long-thin low  $\beta$  expansion is given by:

$$\begin{aligned} \partial/\partial z &\sim \lambda \\ \nabla_T &\equiv \mathbf{e}_x \partial/\partial x + \mathbf{e}_y \partial/\partial y \sim 1 \\ \beta &\sim \lambda^2 \end{aligned} \tag{4}$$

The corresponding expansion for the fields has the form:

$$\begin{aligned} B_z &= B_0 + B_{z2} + \dots \\ B_T &= B_{T1} + B_{T3} + \dots \\ J_z &= J_{z3} + J_{z5} + \dots \\ J_T &= J_{T2} + J_{T4} + \dots \\ P &= P_2 + P_4 + \dots \\ P &= P_2 + P_4 + \dots \\ \kappa_z &= \kappa_{z3} + \kappa_{z5} + \dots \\ \varepsilon_T &= \varepsilon_{T2} + \varepsilon_{T4} + \dots \end{aligned} \tag{5}$$

Here, the subscript "T" refers to the (x,y) rectangular vector components, and the numerical subscripts refer to the order in  $\lambda$  i.e.  $f_n \sim \lambda^n$ .

Before proceeding with the analysis we give a summary of the sequence in which the calculation is carried out.

(1) Leading order:

a) calculate the long-thin vacuum fields

(2) First order in  $\lambda^2$ :

- a) calculate  $B_{z2}$  from transverse pressure balance.
- b) calculate  $J_{\parallel 3}$  from leading order parallel current relation.
- c) calculate  $B_{T3}$  from  $\nabla \cdot \mathbf{B} = 0$  and  $\nabla \times \mathbf{B} = \mathbf{J}$ .
- d) calculate the  $\beta$  and long thin corrections to the field line trajectories, to within a free homogeneous solution, from the magnetic fields.
- e) calculate the free homogeneous solution from the first order parallel current relation.

### III. Analysis

#### A. Leading Order

Substituting the expansion into the starting model leads to the following set of leading order equations:

$$\nabla_T B_0^2 / 2 = 0 \quad (6)$$

$$\nabla_T \cdot \mathbf{B}_{T1} = -\partial B_0 / \partial z \quad (7)$$

$$\mathbf{e}_z \cdot \nabla \times \mathbf{B}_{T1} = J_{z1} = 0 \quad (8)$$

The solution to Eq. (6) - (8) is obtained as follows. Eq. (6) implies that

$$B_0 = B_0(z) \quad (9)$$

The quantity  $B_0(z)$  represents the applied mirror field. Next, from Eq (8)

we can write

$$\mathbf{B}_{T1} = \nabla_T \phi_1 \quad (10)$$

where  $\phi_1(x,y,z)$  is a potential function. Substituting Eq. (10) into Eq. (7)

yields:

$$\nabla_T^2 \phi_1 = -dB_0/dz \quad (11)$$

which has as its solution:

$$\phi_1 = (-r^2/4) dB_0/dz + A r^2/2 \cos 2\theta \quad (12)$$

Here, the first term gives rise to the small component of  $B_r$  associated with the mirror field and the second term is a homogeneous solution describing the applied quadrupole field of amplitude  $A(z)$ .

Converting to rectangular coordinates (x,y) it is straight forward to calculate the vacuum field line trajectories from the magnetic line equations.

$$dx/dz = B_{x1}/B_0$$

$$dy/dz = B_{y1}/B_0 \quad (13)$$

we find

$$x = x_0 \sigma(z) \quad B_{x1}/B_0 = x_0 \sigma' = x \sigma'/\sigma$$

$$y = y_0 \tau(z) \quad B_{y1}/B_0 = y_0 \tau' = y \tau'/\tau \quad (14)$$

where  $x_0$  and  $y_0$  are the coordinates of the field line at the midplane  $z=0$ ,

$B_c = B_0(0)$  is the axial field at the midplane and

$$\sigma(z) = (B_c/B_0)^{1/2} \exp \left[ \int_0^z (A/B_0) dz' \right]$$

$$A/B_c = (\tau \sigma' - \sigma \tau') / 2\sigma^2 \tau^2$$

$$\tau(z) = (B_c/B_0)^{1/2} \exp \left[ -\int_0^z (A/B_0) dz' \right]$$

$$B_0/B_c = 1/\sigma\tau \quad (15)$$

Hereafter, for convenience and in order to facilitate comparison with Pearlstein et al., we express all relationships in terms of  $\sigma(z)$ ,  $\tau(z)$  rather than  $B_0(z)$  and  $A(z)$ . Note that quadrupole symmetry implies that

$$\begin{aligned} B_0(z) &= B_0(-z) \\ \sigma(z) &= \tau(-z) \end{aligned} \tag{16}$$

finally we obtain an expression for the vacuum flux coordinates  $(\psi, \theta_0)$  by observing that the flux surfaces are circles at the midplane,  $z=0$ . Thus, setting  $2\psi/B_c = x^2(0) + y^2(0)$  and  $\tan \theta_0 = y(0)/x(0)$  yields

$$\begin{aligned} \psi / 2 B_c &= x_0^2 + y_0^2 = x^2/\sigma^2 + y^2/\tau^2 \\ \tan \theta_0 &= y_0/x_0 = (\sigma y)/(\tau x) \end{aligned} \tag{17}$$

It is easily verified that the vacuum fields satisfy  $\mathbf{B} = \nabla\psi \times \nabla\theta$

### B. First Order

There are a number of steps required to calculate the  $\beta$  and long thin corrections to the vacuum fields. Following the general sequence previously discussed we begin as follows:

#### 1. Calculate $B_{z2}$

The perturbed axial field  $B_{z2}$  is calculated from the first nonvanishing correction to perpendicular pressure balance:

$$\nabla_T (p_\perp + B_0 B_{z2} + B_{T1}^2/2) - b_T (b_v \cdot \nabla) (B_0^2/2) - B_0^2 (b_v \cdot \nabla) b_T = 0 \tag{18}$$

where  $b_T = (B_{x1}/B_0)\mathbf{e}_x + (B_{y1}/B_0)\mathbf{e}_y$ ,  $b_v \cdot \nabla = \partial/\partial z + b_T \cdot \nabla_T$ .

and for convenience the subscript "2" has been dropped from  $p$ . After some simple rearrangement, Eq. (18) can be rewritten as:

$$\nabla_T [ p_{\perp} + B_0 (B_{z2} - \partial\phi_1 / \partial z) ] = 0 \quad (19)$$

The first term represents the perpendicular particle pressure and the second term represents the magnetic pressure due to the diamagnetic part of the axial field. Eq. (19) can be integrated yielding:

$$B_{z2} / B_0 = 1/B_0 \partial\phi_1 / \partial z - 1/B_0^2 p_{\perp} (\psi, B_0) + f_1(z) \quad (20)$$

The free function  $f_1(z)$  represents a small correction to the applied mirror field. If the conducting wall is moved to infinity then  $f_1(z) = 0$ . Under this assumption,  $B_{z2}/B_0$  can be separated into a  $\beta$  contribution and a long thin contribution as follows:

$$B_{z2} / B_0 = -\beta / B_0^2 + 1/B_0 \partial\phi / \partial z \quad (21)$$

where  $1/B_0 \partial\phi / \partial z = \sigma\tau/2 [ x^2(\sigma' / (\sigma^2\tau))' + y^2(\tau' / (\tau^2\sigma))' ]$

## 2. Calculate $J_3$

The first nonvanishing contribution to  $J$  can be determined from the leading order parallel current relation [Eq. (3)]. It is convenient to carry out the calculation in terms of vacuum flux coordinates,  $(x_0, y_0, l)$

given by:  $x = x_0 \sigma(l)$

$y = y_0 \tau(l)$

$z = l$

(22)



In this system, the operator  $b_v \cdot \nabla = (\partial/\partial l)_{x_0, y_0}$ . Thus, the leading order

contribution to the left hand side of Eq. (3) reduces to

$$b \cdot \nabla Q J_{\parallel} / B^3 \sim \partial/\partial l J_{\parallel} / B_0 \quad (23)$$

The right hand side of Eq. (3) can be evaluated by noting that

$$\begin{aligned} \epsilon_2 &= b_v \cdot \nabla b_T = \epsilon_x x_0 \sigma'' + \epsilon_y y_0 \tau'' \\ \nabla \psi &= B_c [ \epsilon_x (x_0/\sigma) + \epsilon_y (y_0/\tau) ] \end{aligned} \quad (24)$$

$$1/B^2 b \cdot \nabla (p_{\perp} + p_{\parallel}) \times \kappa \sim -x_0 y_0 / B_0 \partial/\partial \psi (p_{\perp} + p_{\parallel}) (\sigma \sigma'' - \tau \tau'')$$

Integrating to obtain  $J_{\parallel 3}$  yields

$$J_{\parallel 3}(x_0, y_0, l) / B_0 = x_0 y_0 \int_1^L dl' / B_0 \partial/\partial \psi (p_{\perp} + p_{\parallel}) (\sigma \sigma'' - \tau \tau'') \quad (25)$$

### 3. Calculate $B_{T3}$

The equations determining  $B_{T3}$  follow from the first order corrections

to  $\nabla \cdot B = 0$  and  $b \cdot (J - \nabla \times B) = 0$ :

$$\partial B_{x3} / \partial x + \partial B_{y3} / \partial y = -\partial B_{z2} / \partial z \quad (26)$$

$$\partial B_{y3} / \partial x - \partial B_{x3} / \partial y = J_{\parallel 3} - b_T \cdot (\nabla \times B)_2 \quad (27)$$

Equations (26) and (27) are solved by writing

$$\begin{aligned} B_{x3} &= \partial \phi_3 / \partial x + \partial A_3 / \partial y + B_0 x [ K(\psi, l) - (\sigma' / \sigma) p_{\perp} / B_0^2 ] \\ B_{y3} &= \partial \phi_3 / \partial y - \partial A_3 / \partial x + B_0 y [ K(\psi, l) - (\tau' / \tau) p_{\perp} / B_0^2 ] \end{aligned} \quad (28)$$

Here  $\phi_3$  and  $A_3$  are scalar and vector potentials to be determined. The terms in the large brackets correspond to part of the particular solution which balances the  $\theta$  independent terms in  $-\partial B_{z2}/\partial z$ . This balancing determines  $K(\psi, l)$ . Substituting into Eqs. (26) and (27) yields the following equations for  $K(\psi, l)$ ,  $\phi_3(x, y, z)$  and  $A_3(x, y, z)$

$$K = 1/(2\psi) \partial/\partial l \int_0^\psi p_\perp / B_0^2 d\psi' \quad (29)$$

$$\nabla_T^2 \phi_3 = -\partial^2 \phi_1 / \partial z^2 \quad (30)$$

$$\nabla_T^2 A_3 = B_0^2 xy / \sigma r \partial S / \partial \psi \quad (31)$$

where

$$S(\psi, l) = -1/B_0 \int_1^L dl' / B_0 (p_\perp + p_\parallel) (\sigma\sigma'' - r r'') - (\sigma^2 - r^2) K \quad (32)$$

The solution for  $\phi_3$  is easily found by substituting  $\phi_1$  from Eq. (12). For boundary conditions we assume that there are no third order sources at infinity (i.e. no  $r^m \cos m\theta$ ,  $r^m \sin m\theta$  terms). This yields

$$\begin{aligned} \phi_3(x, y, z) = & -B_c/64 \left( (r\sigma' + \sigma r') / \sigma^2 r^2 \right)'' r^4 \\ & - B_c/48 \left( (r\sigma' + \sigma r') / \sigma^2 r^2 \right)'' r^4 \cos 2\theta \end{aligned} \quad (33)$$

The solution to Eq. (31) is somewhat more complicated. For  $A_3$  regular at infinity, the solution has been given by Pearlstein, et. al., using a Greens function technique. Also, for convenience their calculation is

carried out in vacuum flux coordinates  $(x_0, y_0, l \leftrightarrow \psi, \theta_0, l)$  rather than Eulerian coordinates  $(x, y, z)$ . The result is

$$A_3(x_0, y_0, l) = -2/(\mu B_0(\sigma + \tau)^2)$$

$$\text{Im} \int_0^\psi d\psi' S(\psi', l) \left(1 + 4\psi'/\psi [\mu e^{2i\theta_0}/(1 - \mu e^{2i\theta_0})^2]\right)^{-1/2}$$

(34)

where  $\mu = (\tau - \sigma)/(\tau + \sigma)$ ,  $2\psi/B_c = x_0^2 + y_0^2$ ,  $\tan \theta_0 = y_0/x_0$ .

At this point in the calculation the  $\beta$  and long thin corrections to the magnetic field have been completely determined:  $B_{z2}$  from Eq. (21), and  $B_{x3}$  and  $B_{y3}$  from Eq. (28) with  $K$ ,  $\Phi_3$  and  $A_3$  given by Eqs. (29), (33) and (34).

#### 4. Calculate $\psi$ and $\theta_0$

The final step in the analysis is to calculate the  $\beta$  and long thin corrections to the flux coordinates. In particular we wish to determine the modifications to the vacuum flux surfaces. This slightly lengthy calculation can be carried out as follows. To begin, we expand the vacuum field line trajectories as

$$x = x_v + \xi$$

$$y = y_v + \eta$$

$$z = l$$

(35)

where  $x_v = x_0\sigma(1)$ ,  $y_v = y_0\tau(1)$  and  $\xi(x_0, y_0, 1)$ ,  $\eta(x_0, y_0, 1)$  are small corrections due to  $\beta$  and long thin effects. We assume  $\xi/x_v \sim \eta/y_v \sim \lambda^2$ .

Since the magnetic field is known,  $\xi$  and  $\eta$  can be determined by solving the field line trajectory equations:

$$\begin{aligned} dx/dl &= B_x / B_z \\ dy/dl &= B_y / B_z \end{aligned} \quad (36)$$

to next order in  $\lambda^2$ . We find:

$$\begin{aligned} \partial/\partial l (\xi/\sigma) &= R_\xi \\ \partial/\partial l (\eta/\tau) &= R_\eta \end{aligned} \quad (37)$$

$$\begin{aligned} R_\xi(x_0, y_0, 1) &= (1/\sigma B_0) \left( \partial\Phi_3/\partial x - (x\sigma'/\sigma) \partial\Phi_1/\partial z \right) + 1/B_c \partial A_3/\partial y_0 + x_0 K(\psi, 1) \\ R_\eta(x_0, y_0, 1) &= (1/\tau B_0) \left( \partial\Phi_3/\partial y - y\tau'/\tau \partial\Phi_1/\partial z \right) - 1/B_c \partial A_3/\partial x_0 + y_0 K(\psi, 1) \end{aligned} \quad (38)$$

In Eq. (38) the terms in the bracket are to be expressed in terms of vacuum flux coordinates,  $x = x_0\sigma$ ,  $y = y_0\tau$ ,  $z = 1$ . The quantities  $R_\xi$  and  $R_\eta$  are known functions. Thus, Eq. (37) can be integrated, yielding

$$\begin{aligned} \xi(x_0, y_0, 1) &= \sigma \int_0^1 R_\xi(x_0, y_0, l') dl' + \sigma \bar{\xi}(x_0, y_0) \\ \eta(x_0, y_0, 1) &= \tau \int_0^1 R_\eta(x_0, y_0, l') dl' + \tau \bar{\eta}(x_0, y_0) \end{aligned} \quad (39)$$

where  $\bar{\xi}$  and  $\bar{\eta}$  are two free functions of integration to be determined shortly.

The next step in the calculation is to express the flux coordinates in terms of  $\xi$  and  $\eta$ . If we focus on a flux surface whose vacuum labels are

given by  $2\psi/B_c = x_0^2 + y_0^2$ ,  $\tan \theta_0 = y_0/x_0$ , then this flux surface, in presence of  $\beta$  and long thin corrections is given by

$$2\psi/B_c = x_0^2 + y_0^2 = \left( (x - \xi)/\sigma \right)^2 + \left( (y - \eta)/\tau \right)^2$$

$$\tan \theta_0 = y_0/x_0 = \sigma(y - \eta)/\tau(x - \xi) \quad (40)$$

For small  $\xi$  and  $\eta$

$$2\psi/B_c \sim x^2/\sigma^2 + y^2/\tau^2 - 2x\xi/\sigma^2 - 2y\eta/\tau^2 \quad (41)$$

$$\tan \theta_0 \sim \sigma y/\tau x (1 + \xi/x - \eta/y) \quad (42)$$

Note that in Eq. (41),  $\xi$  and  $\eta$  can be expressed to the order required as:

$$\xi(x_0, y_0, 1) \sim \xi(x/\sigma, y/\tau, z), \quad \eta(x_0, y_0, 1) \sim \eta(x/\sigma, y/\tau, z)$$

A further relation of interest is the equation for the  $z=0$  midplane flux surface. From Eqs. (39) and (41) we find

$$2\psi(x, y, z=0)/B_c = x^2 + y^2 - 2x\bar{\xi}(x, y) - 2y\bar{\eta}(x, y) \quad (43)$$

Thus, what remains in the calculation of  $\psi$  and  $\theta_0$  is the determination of the free functions  $\bar{\xi}(x_0, y_0)$ ,  $\bar{\eta}(x_0, y_0)$ . The first relation between  $\bar{\xi}$  and  $\bar{\eta}$  arises from the assumption that  $\psi$  and  $\theta_0$  are legitimate flux coordinates; that is,  $\psi$  and  $\theta_0$  must satisfy  $\mathbf{E} = \nabla\psi \times \nabla\theta_0$ . Since the fields have already been determined, a comparison of the left and right sides of this equation should be a verification of the self consistency of the algebra. Upon carrying out the comparison, we find that the  $x$  and  $y$  components exactly balance and that the  $z$  component leads to the relation

$$1/\sigma \partial \bar{\xi} / \partial x_0 + 1/\tau \partial \bar{\eta} / \partial y_0 = -B_{z2}/B_0 \quad (44)$$

The particular solution to  $\xi$  and  $\eta$  [see Eq. (39)] balance the  $B_{z2}/B_0$  term and we are left with a constraint relation between  $\bar{\xi}$  and  $\bar{\eta}$ .

$$\partial\bar{\xi}/\partial x_0 + \partial\bar{\eta}/\partial y_0 = 0 \quad (45)$$

From Eq. (45) we can introduce a stream function  $\bar{\chi}(x_0, y_0)$  such that

$$\bar{\xi} = \partial\bar{\chi}/\partial y_0, \quad \bar{\eta} = -\partial\bar{\chi}/\partial x_0 \quad (46)$$

Introducing cylindrical flux coordinates  $(r_0, \theta_0)$  defined by

$$\begin{aligned} x_0 &= r_0 \cos \theta_0 \\ y_0 &= r_0 \sin \theta_0 \end{aligned} \quad (47)$$

we find that the midplane flux surface [Eq. (43)] simplifies to

$$2\psi(x_0, y_0, 0)/B_c = r_0^2 - 2\partial\bar{\chi}/\partial\theta_0 \quad (48)$$

The second relation between  $\bar{\xi}$  and  $\bar{\eta}$  arises from the  $\beta$  and long thin corrections to the parallel current relation. Specifically, the corrections to Eq. (3) gives an equation for  $\partial J_{\parallel}/\partial l$  in terms of previously determined lower order quantities (including  $\bar{\xi}$  and  $\bar{\eta}$ ). The boundary condition that  $J_{\parallel}$  vanish across each end of the machine imposes a constraint on the lower order solutions and it is this constraint that leads to the second relationship between  $\bar{\xi}$  and  $\bar{\eta}$ . The exact unexpanded form of the parallel current constraint is given by

$$C \equiv \int_{-L}^{+L} ds/B^2 \mathbf{b} \cdot \nabla (p_{\perp} + p_{\parallel}) \times \mathbf{z} = 0 \quad (49)$$

where  $s$  is arc length along the magnetic field.

The leading order contribution to Eq. (49) is of fourth order in  $\lambda$  and vanishes by symmetry. The first non-vanishing contribution is of sixth order. After a straightforward but tedious calculation, this correction can be calculated and set to zero. This yields the final relation for  $\bar{\chi}$  which can be expressed as

$$\Pi \frac{\partial^2 \bar{\chi}}{\partial \theta_0^2} + \Sigma_\beta + \Sigma_\lambda = 0 \quad (50)$$

Here  $\Pi$  is a constant governing low  $\beta$  flute stability

$$\Pi = \int_{-L}^{+L} dl/B_0 \frac{\partial p}{\partial \psi} (\sigma\sigma'' + \tau\tau'') \quad (51)$$

with  $p(\psi, B_0) = (p_\perp + p_\parallel)/2$ . The quantity  $\Sigma_\beta$ , first calculated by Pearlstein, et al., represents the flux surface distortion due to the  $\beta$  corrections.

$$\begin{aligned} \Sigma_\beta(r_0, \theta_0) = & \int_{-L}^{+L} dl/B_0 \frac{\partial p}{\partial \psi} \left( (\sigma\sigma'' + \tau\tau'') \int_0^1 dl' \frac{\partial^2 A}{\partial \theta_0^2} \right. \\ & + (\sigma\sigma'' - \tau\tau'') \int_0^1 dl' \frac{\partial}{\partial \theta_0} (r_0 \sin 2\theta_0 \frac{\partial}{\partial r_0} + \cos 2\theta_0 \frac{\partial}{\partial \theta_0}) A \\ & + [(\sigma^2 - \tau^2)(r_0 \cos \theta_0 \frac{\partial A}{\partial r_0} - \sin 2\theta_0 \frac{\partial A}{\partial \theta_0}) \\ & \left. - (\sigma^2 + \tau^2) r_0 \frac{\partial A}{\partial \theta_0} \right] \end{aligned} \quad (52)$$

and  $A = A_3/B_c$ .

The quantity  $\Sigma_\lambda$  describes the flux surface distortion due to long thin corrections and it is this term which extends the results of Pearlstein, et al. We find

$$\Sigma_\lambda(r_0, \theta_0) =$$

$$1/8 r_0^4 \sin 4\theta_0 \int_{-L}^{+L} dl/B_0 \left( A_1(B_0 \partial^2 p / \partial \psi \partial B_0) + A_2 \partial p / \partial \psi \right) \quad (53)$$

where  $A_1$ , and  $A_2$  are functions of  $l$  alone, given by

$$A_1 = -(\sigma\sigma'' - r r'') (f_0 + \sigma^2 - r^2)$$

$$A_2 = (\sigma\sigma'' - r r'') [f_0 + 4(\sigma^2 - r^2)]$$

$$+ 2(\sigma' r'' - r' \sigma'') (\tau\sigma' - \sigma r')$$

$$+ [(\sigma\sigma' - r r') f_0 + g_0 (\sigma^2 - r^2)^2 + g_e (\sigma^4 + r^4)]$$

$$+ 4\sigma\sigma'' \int_0^1 [(\sigma'/\sigma) f_0 + (\sigma^2 - r^2) g_0 + \sigma^2 g_e] dl'$$

$$- 4r r'' \int_0^1 [(r'/r) f_0 + (\sigma^2 - r^2) g_0 + r^2 g_e] dl'$$

with

$$f_0 = \sigma\tau [ \sigma^2 (\sigma'/\sigma^2 \tau)' - r^2 (r'/\sigma r^2)' ]$$

$$g_0 = \sigma\tau/8 \left( (\tau\sigma' + \sigma r') / \sigma^2 r^2 \right)''$$

$$g_e = \sigma\tau/6 \left( (\tau\sigma' - \sigma r') / \sigma^2 r^2 \right)''$$



Observe that the long thin corrections introduce a pure fourth harmonic correction to the flux surfaces.

#### IV. Applications

In this section we derive analytical expressions for  $\Sigma_\lambda$  and  $\Sigma_\beta$  using certain simplifying assumptions. We then apply these expressions to describe the equilibrium of actual mirror experiments. If we assume

$$\begin{aligned}\sigma &= e^{cz} R^{-1/2}(z) \\ \tau &= e^{-cz} R^{-1/2}(z)\end{aligned}\tag{54}$$

with a mirror ratio  $R(z) \equiv B_0/B_c = 1 + (R_0 - 1)z^2/L^2$  and assume  $cL \gg 1$ , (values of  $c$  and  $L$  for three magnetic geometries are given in Table 1.) then the largest terms in (53) are

$$\begin{aligned}A_1(1) &\sim -\sigma\sigma''\sigma^{-2} \sim -c^4 e^{4cl}/R^2 \\ A_2(1) &\sim 4\sigma\sigma''\sigma^{-2} \sim 4c^4 e^{4cl}/R^2\end{aligned}\tag{55}$$

with all other terms smaller by at least a factor of  $1/Lc$ . A comparison of these analytical expression with the exact computer generated functions  $A_1$  and  $A_2$  is given in figure 1., and shows close agreement.

To evaluate (53) we assume a separable pressure profile:

$$p(\psi, B) = \Psi(\psi) \hat{P}(B_0)\tag{56}$$

where  $\hat{P}(B_0)$  vanishes at the mirror throat, but  $d\hat{P}(B_0)/dB_0|_{B_{\max}} \equiv \hat{P}'_m \neq 0$ .

Using the expansion

$$\hat{P}(B_0) = \hat{P}'_m (B_0 - B_{\max}) \quad (57)$$

with  $\hat{P}'_m < 0$ , and substituting (54), (55) and (56) into (53) we find:

$$\Sigma_\lambda(r_0, \theta_0) = -1/(16 R_0^2) c^3 r_0^4 e^{4cL\psi} \hat{P}'_m \sin 4\theta_0 \quad (58)$$

If we assume a linear pressure profile

$$\psi(\psi) = 1 - \psi/\psi_B \quad (59)$$

then

$$\Sigma_\lambda(r_0, \theta_0) = 1/(16 R_0^2) c^3 r_0^4 e^{4cL} \hat{P}'_m \sin 4\theta_0 \quad (60)$$

Using the pressure profiles (57) and (59) and magnetic field profile (54) as well as the  $Lc \gg 1$  assumption we now find an analytical expression for  $\Sigma_\beta$ . Our starting point is Eq. (B7) of Pearlstein et. al. with a minor typographical error corrected. Using  $Lc \gg 1$  gives  $k_1(z) \gg k_2(z)$ :

$$k_1(z) \sim 4\hat{P}'_m c^2 (R_0 - 1)/(B_0 \sigma^2 R_0^2) \int_z^L dz' (1 - z'^2/L^2) e^{2cz'} \quad (61)$$

where the large exponent allows the substitution of the constant  $R_0$  for  $R(z)$ . Substituting (61) into

$$\Sigma_{\beta} \sim 8\psi^2 / (3B_c \psi_B^2) \sin 4\theta_0 \int_0^L dz \hat{P}_{\sigma\sigma} / B \int_0^z dz' k_1(z') \quad (62)$$

we obtain

$$\Sigma_{\beta} \sim -r_0^4 \sin 4\theta_0 e^{4cL} (\hat{P}_m')^2 (R_0 - 1)^2 / (3\psi_B^2 c R_0^4 L^2) \quad (63)$$

Because  $\hat{P}_m' < 0$ ,  $\Sigma_{\lambda}$  and  $\Sigma_{\beta}$  are of the same sign and add. Comparing the magnitudes of  $\Sigma_{\lambda}$  and  $\Sigma_{\beta}$ , we find

$$| \Sigma_{\beta} / \Sigma_{\lambda} | = 16\hat{P}_m' (R_0 - 1)^2 / (3\psi_B^2 c^4 L^2 R_0^2) \quad (64)$$

Note that the ratio scales with  $\beta$ , so  $\Sigma_{\lambda}$  is much more important than  $\Sigma_{\beta}$  at low  $\beta$ . In the Constance mirror,  $L \sim 40$  cm.,  $c \sim 0.069$  cm.<sup>-1</sup>,  $R_0 = 2$ , and if we use the approximation  $\hat{P}_m' \sim -\beta B_c$  then

$$| \Sigma_{\beta} / \Sigma_{\lambda} |_{\text{Constance}} \sim 2.5\beta \quad (65)$$

In Constance the  $\beta$  in the core plasma is no more than 10%-15%, so  $\Sigma_{\lambda}$  is dominant everywhere in the machine.

We have now calculated all the terms in Eq. (48) except the interchange stability constant  $\Pi$ . Using the same pressure and field profiles Eq. (51) yields

$$\Pi \sim 2c^2 \int_0^L dz \hat{P}_m' (B_0 - B_{\max}) \psi' e^{2cz} / (B_0 R) \quad (66)$$

$$\Pi \sim \hat{P}_m (R_0 - 1) e^{2cL} / (R_0 \psi_B L) \quad (67)$$

Note that here, as in the calculation of  $\Sigma_\lambda$  and  $\Sigma_\rho$ , the large exponential allows the substitution of  $R_0$  for the function  $R$  in the denominator, simplifying the integral.

Combining equations (48), (58), (63) and (67) the midplane flux surface is:

$$\psi(r_0, \theta_0) = B_c r_0^2 / 2 \left( 1 - r_0^2 / 2 \cos 4\theta_0 e^{2cL} [Lc^3 / (16R_0) + 2(R_0 - 1)\beta / (3r_B^2 LcR_0^3)] \right) \quad (68)$$

where  $r_B = (2\psi_B / B_c)^{1/2}$  is the radius at which the pressure vanishes.

## V. Comparison with Codes

In this section we compare our calculated equilibrium with two equilibrium codes, the VEPEC 3D code and the new "Long Thin Equilibrium" (LTE) code at Livermore.<sup>4</sup>

We have evaluated  $\Sigma_\lambda$  and  $\Sigma_\beta$  for three magnetic geometries: the Constance-B mirror, the anchor of the TARA tandem mirror at MIT, and a modified IIX-IIB coil set used by the groups at Livermore to benchmark their codes. The parameters of each machine are shown in Table 1. We obtain the results in this section by numerically evaluating Eqs. (53) and (65), but throughout we have found that the simple analytic expressions (63), (66) and (71) agree with our numerical evaluations within a factor of 2.

Figure 2. shows the amplitude of the long-thin quadrupole distortion to the midplane flux surface as a function of normalized flux for Constance. The quantity  $A_{4\lambda}/A_0$  is plotted, where the equation of the flux surface is

$$r^2(\psi, \theta) = A_0(\psi) + [A_{4\lambda}(\psi) + A_{4\beta}(\psi)] \cos 4\theta \quad (69)$$

The two lines in the figure show the long-thin contribution to the quadrupole distortion for a pressure profile which drops to zero only part of the way up the mirror. The  $z$  location where the pressure vanishes was chosen as the electron cyclotron resonance location for two typical values of magnetic field. This pressure profile corresponds more closely

with what is found experimentally in Constance than the profile of eq. (57), and also leads to reasonable values of  $A_{4\lambda}/A_0$ . If the pressure is continued all the way to the mirror peak, an unphysically large value of  $A_{4\lambda}/A_0$  results. This is due to the fact that the fanning region of Constance is not well described by the long-thin approximation, and thus the long-thin expansion on which our theory is based breaks down if much pressure extends into this region. Figure 3. shows typical Constance flux surfaces obtained with our theory. For this graph the core  $\beta = 15\%$  is assumed.

Figures 4. and 5. are plots of the quadrupole distortions for the TARA anchor and the IIX-IIB . A core  $\beta$  of 15% is assumed in each case, and this finite  $\beta$  contribution is shown separately and may be compared with the long-thin contribution of the vacuum field, which is also graphed.

The weighting of the pressure against the exponential fanning of the field lines and curvature in eqs. (51), (53) and (62) implies that our results are very sensitive to the exact axial pressure profile. As an example, if the pressure in the IIX-IIB case extends to only 40 cm. instead of the the full 75 cm., we find that the flux surface distortions are smaller by a factor of 15. Thus in comparing our results to equilibrium codes we do not expect numerical agreement to better than a factor of 2 or 3, and instead we look at the scaling with  $\beta$ .

The VEPEC code results for Constance are shown in figure 6. Note that there is a significant distortion even at very low  $\beta$ , which scales linearly with flux. Although the magnitude of the distortion is lower than we predict by a factor of about 3, the existence of distortions at vanishing pressure and

the scaling with flux are in agreement with the predictions of our analytic equilibria including the new long-thin terms.

The results obtained with the LTE code are shown in figure 7. The  $\beta$  corrections are smaller than we predict by a factor of 3. The long-thin corrections are not part of the physics which is included in the code, so we see only corrections which scale linearly with  $\beta$ .

The results of both the VEPEC and LTE codes are at this time open to question. Benchmarking of the codes continues, and as of this writing, whether VEPEC converges for very long-thin geometries is still uncertain.

## VI. Conclusions.

We have derived an analytic equilibria for a tandem mirror with quadrupole symmetry which extends the results of Pearlstein, et. al. In some cases the new long-thin corrections are shown to be larger than the finite  $\beta$  corrections, making the flux surfaces more diamond shaped than previously thought. Using model field and pressure profiles, we have derived simple analytic expressions for the corrections and flux surfaces.

We applied the theory to three magnetic field geometries and calculated the quadrupole flux surface distortions. These were compared with two equilibrium codes and agreement was found for flux surface shapes and  $\beta$  scaling. In particular, the VEPEC code showed quadrupole distortions at low  $\beta$ , which agrees with our predictions.

## Acknowledgments

We thank L.D. Pearlstein for helpful discussions, and D. Anderson for furnishing VEPEC code results. One of (D.G.) is supported by the Fannie and John Hertz Foundation.



## References

1. L.D. Pearlstein, T.B. Kaiser, and W.A. Newcomb, Phys. Fl. 24, 1326 (1981)
2. L.D. Pearlstein, T.B. Kaiser, and W.A. Newcomb, Phys. Fl. 27, 2781 (1984)
3. D.V. Anderson, J. Breazeal, and C.B. Sharp, J. Comp. Phys. 46, 189 (1982)
4. L.D. Pearlstein, private communication.

Machine	L	c	Plasma radius
	(cm.)	(cm. <sup>-1</sup> )	(cm.)
Constance-B	40	.069	10
TARA Anchor	50	.03	15
IIX-IIB	75	.032	3

Table 1.

L = 40. C = 0.069

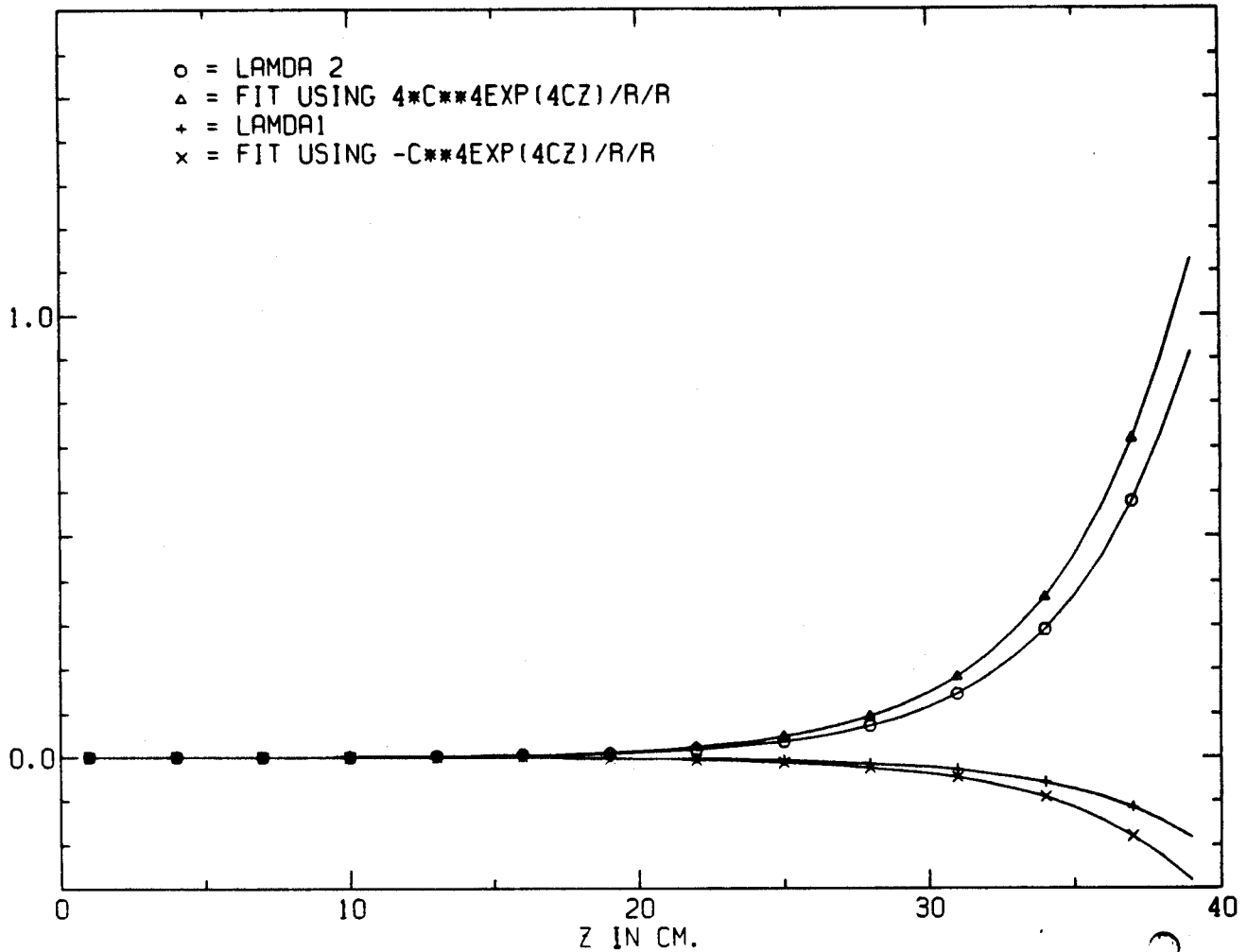


Figure 1. A comparison of the analytic expressions for  $A_1$  and  $A_2$  versus the exact computer generated functions shows close agreement. Constance parameters were used.

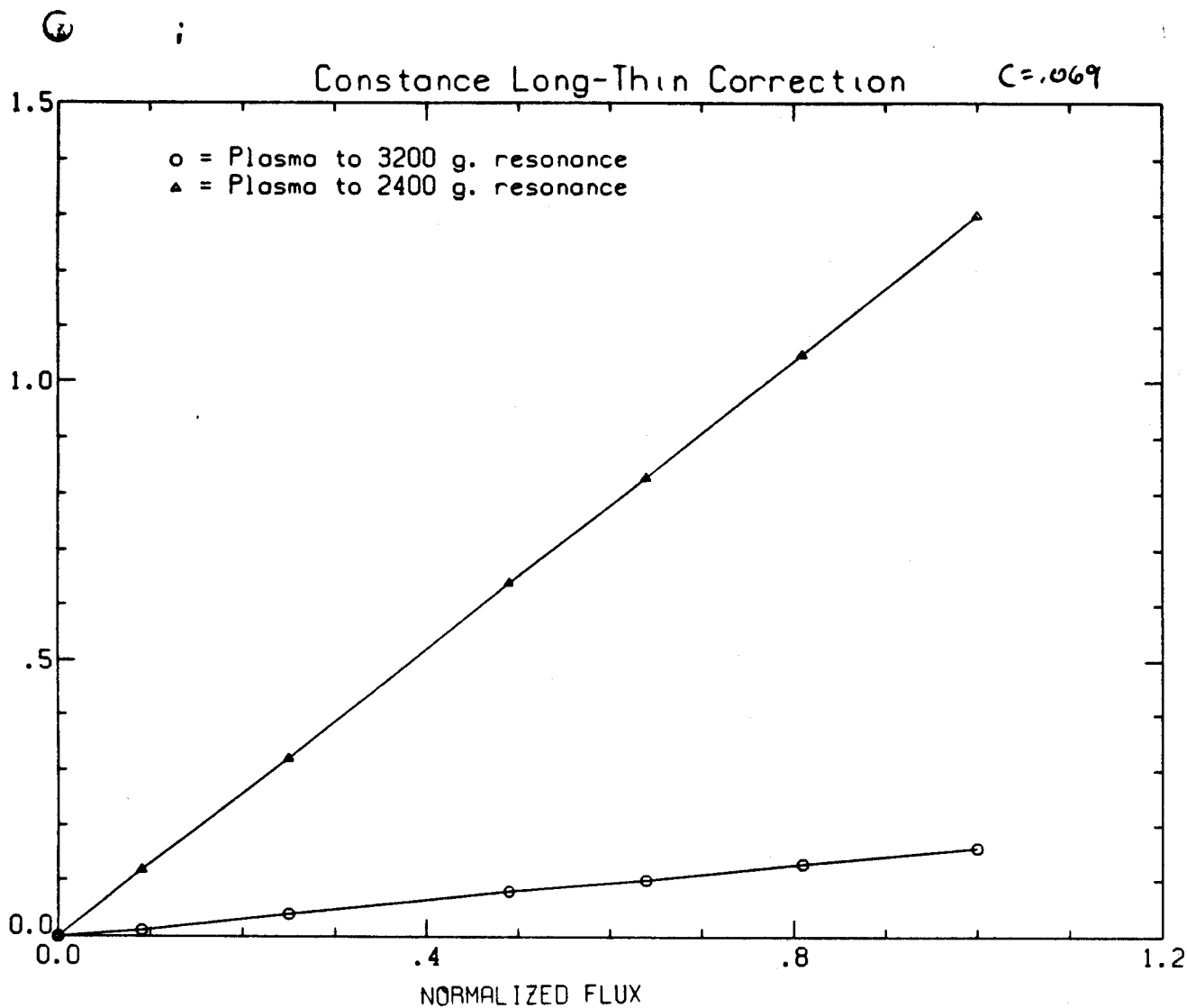


Figure 2a. The long-thin contribution to the quadrupole distortion of the Constance midplane flux surface as calculated in our theory. The two lines show the value of  $A_{4\lambda}/A_0$  for cases where the pressure extends only part of the way up the mirror. The top line has a pressure cut-off at 25 cm. and the bottom line has a cut-off at 17 cm. These values are the position of the electron cyclotron resonance location for two typical operating magnetic fields.

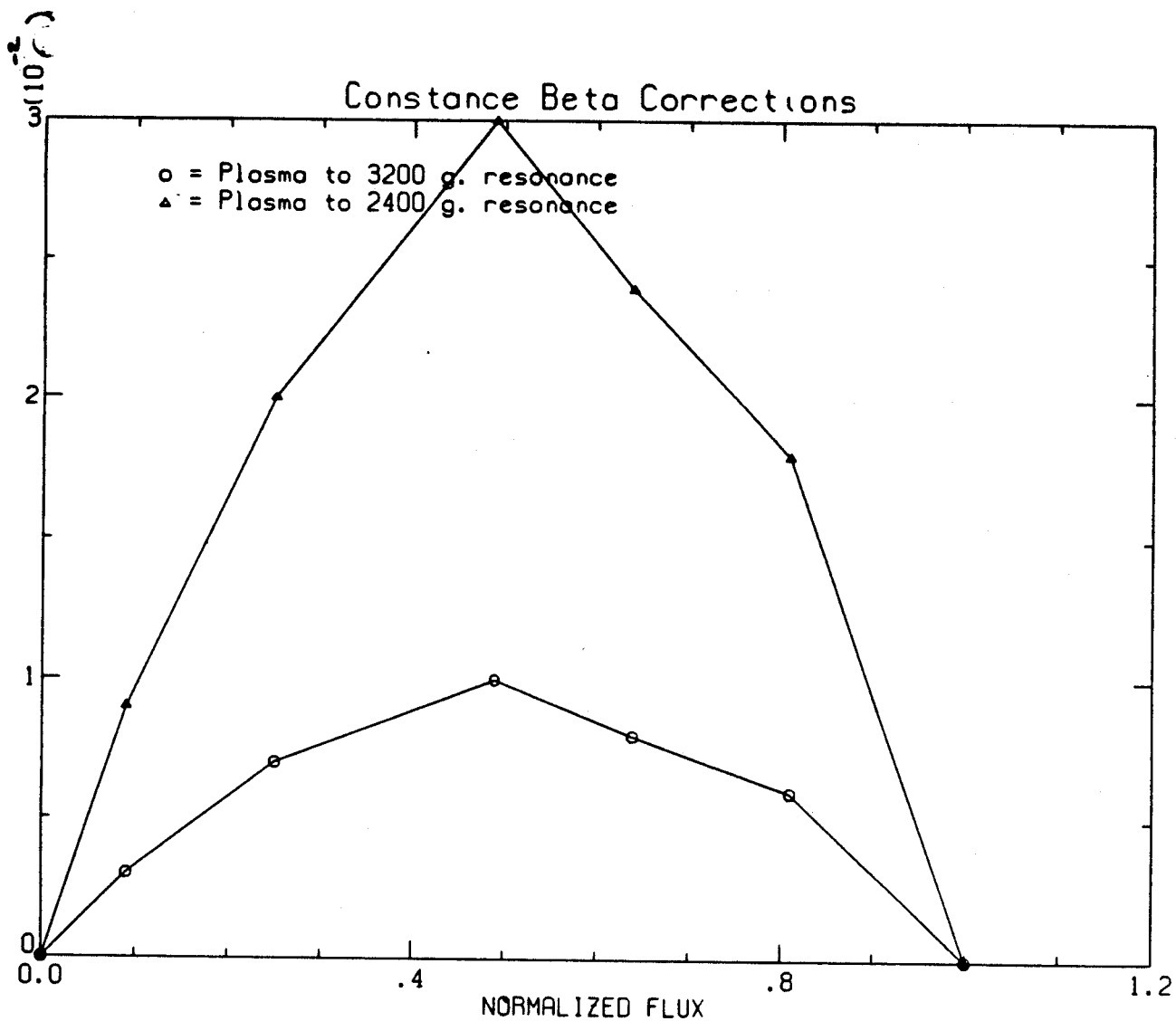
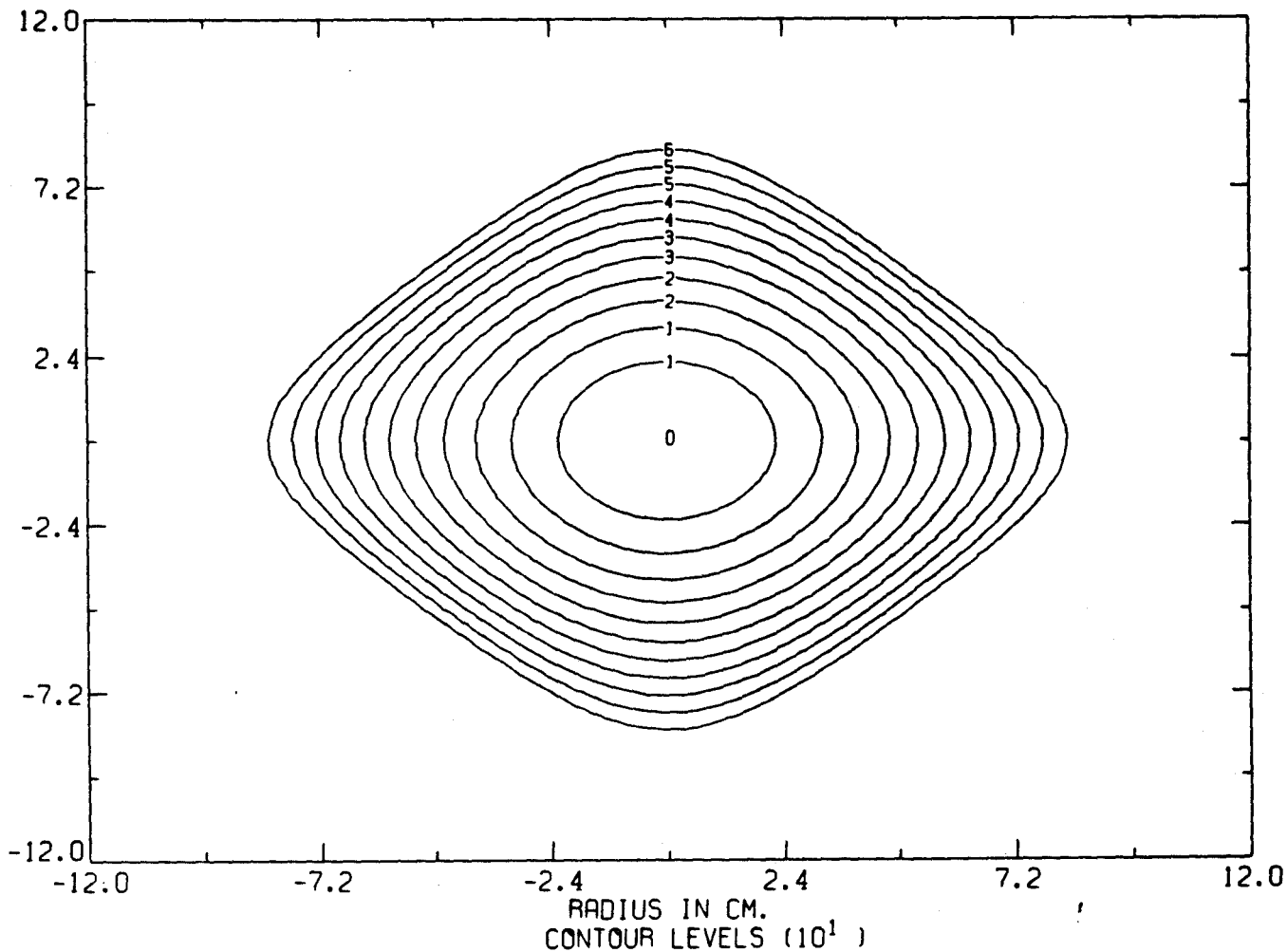


Figure 2b. The beta contribution to the quadrapole distortion of the Constance midplane flux surface is much smaller than the contribution due to the long-thin term in our theory. The two curves correspond to the same pressure profiles as in figure 2a.

# FLUX SURFACES



1988 Tokamak Mirror Experiment M.I.T. Plasma Fusion Center 21-FEB-88 15:13 PAGE 1

Figure 3. Typical Constance midplane flux surfaces as calculated from our theory. Note that the distortion is diamond shaped.

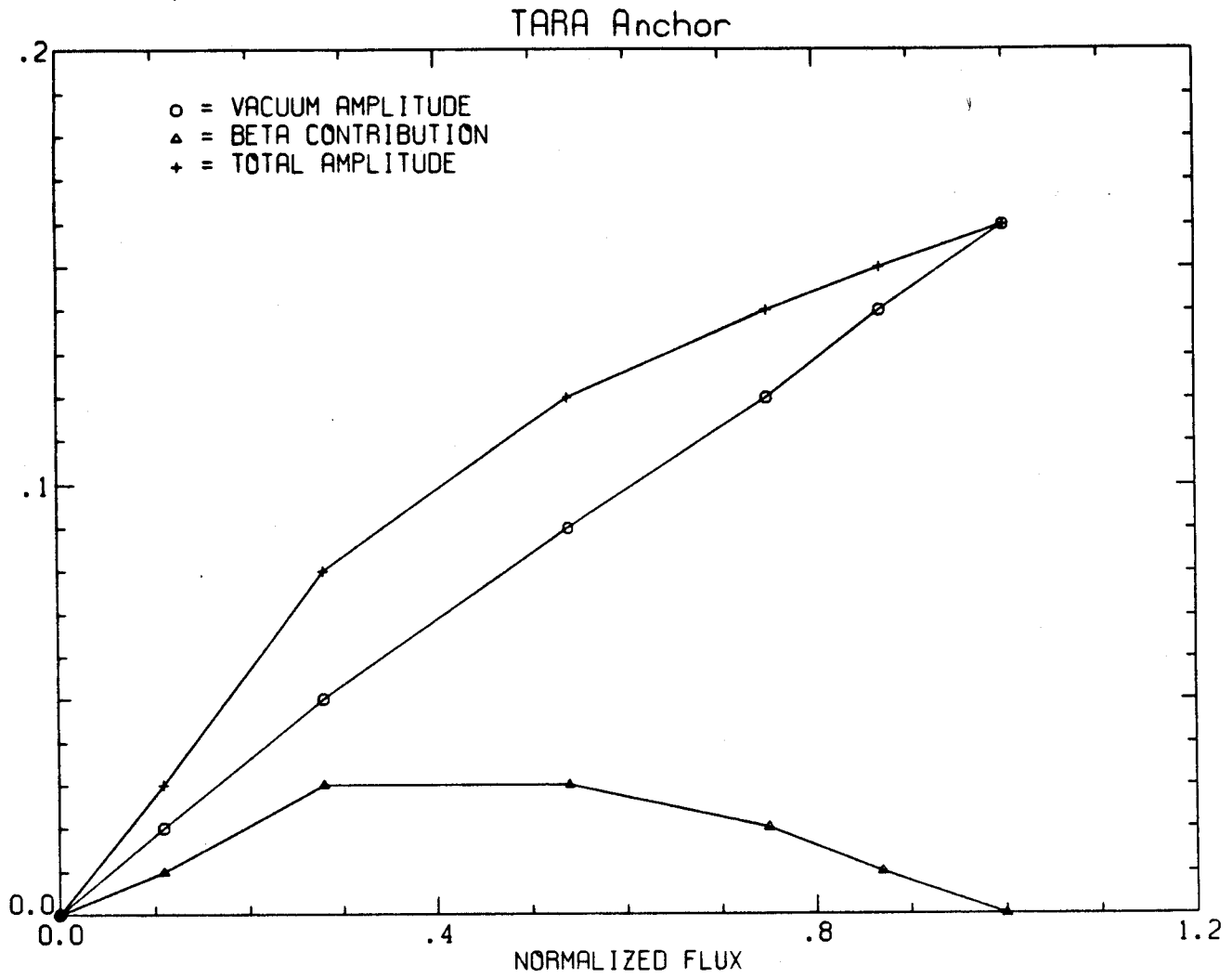


Figure 4. Quadrupole distortions for TARA anchor.  $\beta = 15\%$ .

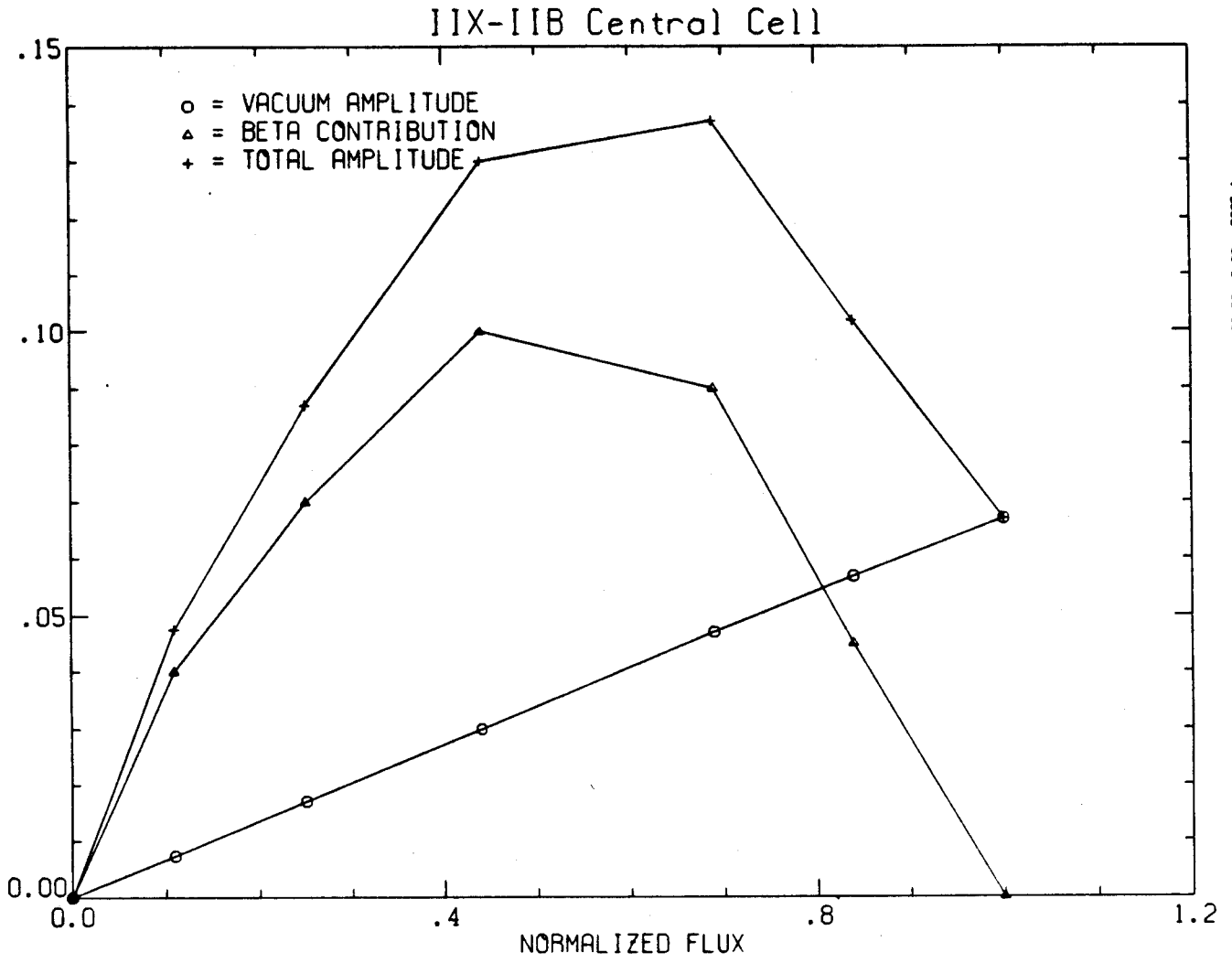


Figure 5. Quadrupole distortions for IIX-IIB central cell.  $\beta = 15\%$ .



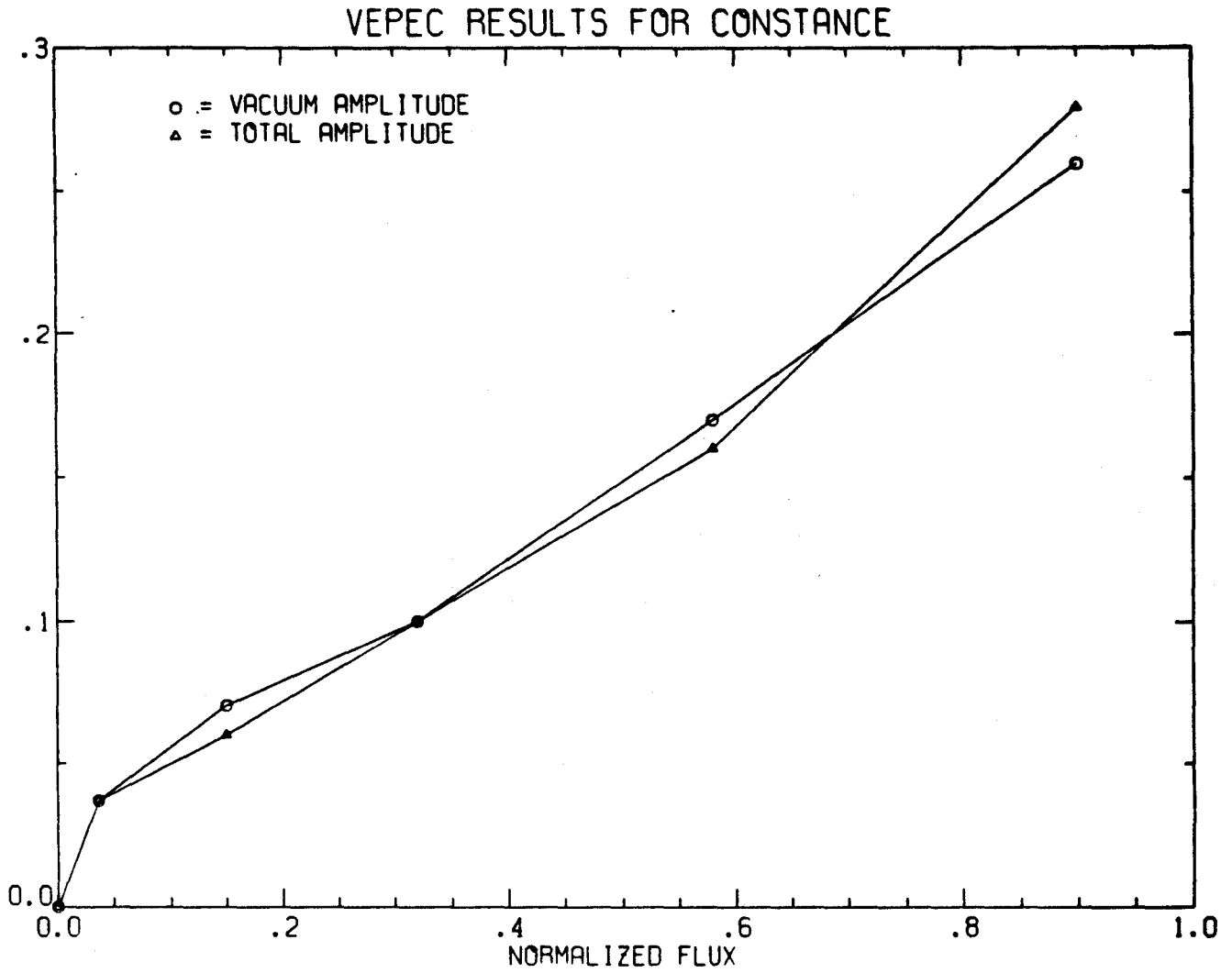
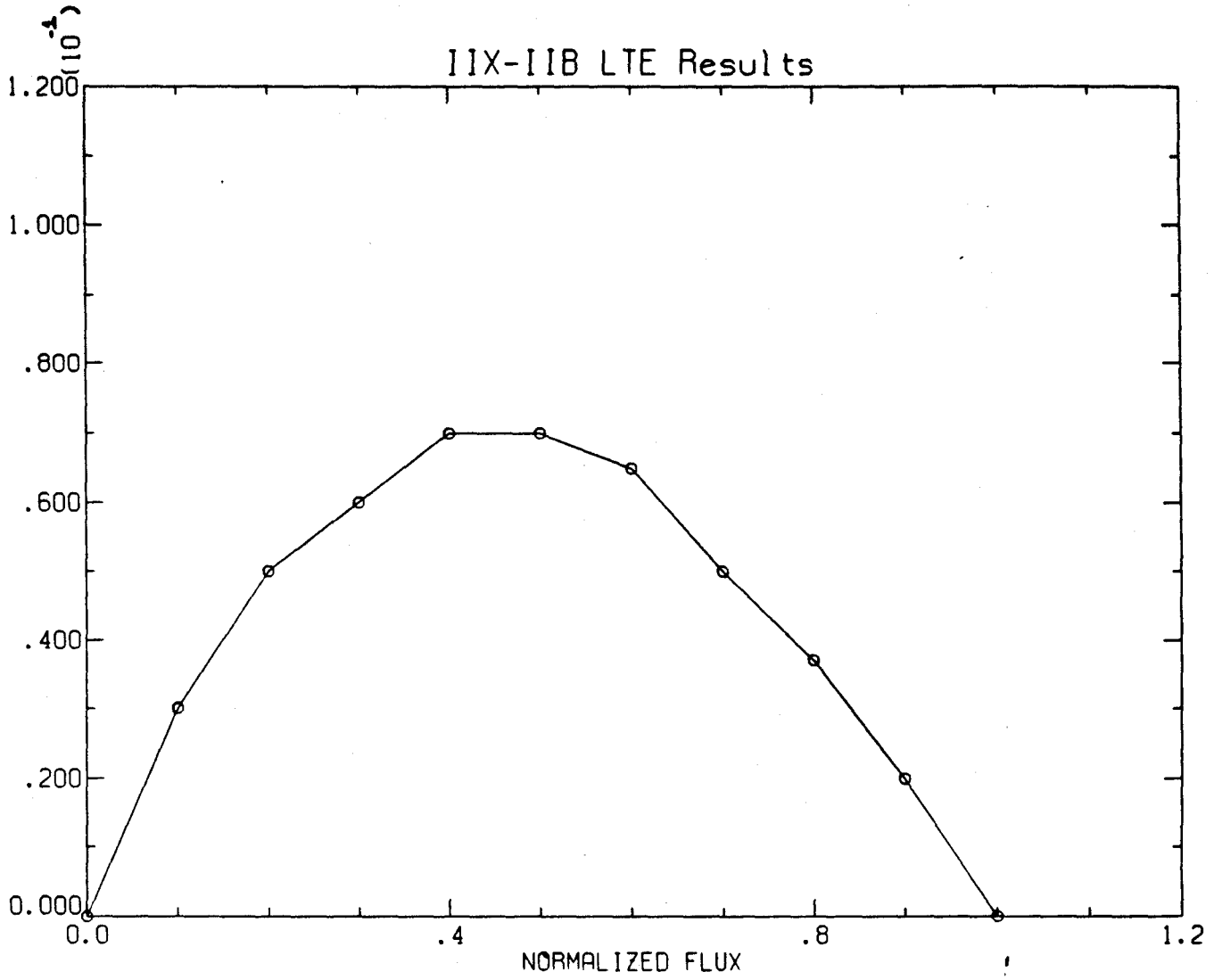


Figure 6. VEPEC code shows definite vacuum contribution which scales linearly with flux. In fact the finite  $\beta$  contribution ( $\beta = 15\%$ ) is barely visible.



1999 London Mirror Experiment M. I. I., Plasma Fusion Center 11-09-95 17:00 PAGE 1

Figure 7. LTE code shows a smaller  $\beta$  than we find for IIX-IIB.